University of Groningen

Fundamental limitations of THz and Niobiumnitride SIS mixers

Dieleman, Pieter

IMPORTANT NOTE: You are advised to consult the publisher's version (publisher's PDF) if you wish to cite from it. Please check the document version below.

Document Version
Publisher's PDF, also known as Version of record

Publication date:
1998

Citation for published version (APA):
Dieleman, P. (1998). *Fundamental limitations of THz and Niobiumnitride SIS mixers*. [Thesis fully internal (DIV), University of Groningen]. University of Groningen.

Chapter 3

Performance analysis of Nb junctions at 800–1000 GHz

We study the gain and noise of a receiver consisting of a niobium junction embedded in an aluminum impedance matching circuit. The junction is operated in a waveguide mount with an adjustable backshort. The uncorrected double side band noise temperatures are 940 K to 1388 K for 820 to 980 GHz respectively. The total optical loss is obtained from the losses of the individual components, the losses in the stripline are calculated using the Reuter-Sondheimer equation in the extreme anomalous limit. The embedding impedance follows from the pumped curves and the Tucker equations which are also used to determine the noise and gain of the junction. The main limitation to the receiver sensitivity is shown to be the loss in the aluminum circuit.

3.1   Introduction

Heterodyne mixers incorporating Superconductor-Insulator-Superconductor (SIS) tunnel junctions have proven to be sensitive receivers for radio astronomy. As application of these devices shifts from the millimeter into the submillimeter wavelength regime, the use of classical mechanical tuning systems becomes more cumbersome. Employing integrated tuning elements[1] has greatly extended the upper frequency limit and bandwidth of the SIS receiver. This induced investigations to establish the intrinsic upper frequency limit of the mixer[2], [3]. It is clear from

theory[4] that a SIS junction can be used for mixing at frequencies up to twice the gap frequency ($f_{gap} = 2\,\Delta/h$, in which Δ is the superconductor energy gap). However, already at frequencies above 800 GHz the sensitivity of the device decreases considerably[5]. Analysis of the receivers shows that microwave losses due to dissipation in the niobium integrated tuning structure limit the performance [6]. The losses can be reduced by using a highly conductive normal metal such as aluminum for the tuning structure[7],[8],[9]. The aim of the present analysis is to determine the main contributions to the noise temperature in SIS receivers employing Al striplines at THz frequencies. In this article the layout of the mixer will be described, the noise and loss contributions of the separate parts of the receiver will be estimated and the measured receiver noise is compared with the calculated values. The results will be discussed and possible improvements to the receiver system are proposed

3.2   Receiver configuration

The Nb junctions used are fabricated by sputtering on 200 μm thick fused quartz substrates. The junction has an area of 1 μm^2 and a normal resistance R_N of 56 Ω. An I,V curve measured at 4.5 K is shown in Fig. 3.2a. The subgap- to normal resistance ratios, $R_{(2mV)}/R_N$ are 25 and 114 at 4.5 and 3 K resp. The endloaded stripline consists of a UHV evaporated Al bottom layer, sputtered SiO$_2$ as the dielectric and a sputtered top Al layer. The width of the stripline is 10 μm, the length is 48 μm. The residual resistance ratio defined as $R_{(300K)}/R_{(5K)}$ of the evaporated Al is 10, the sputtered layer has a ratio of 5. The details of the process are described in [10]. The substrate is polished down to 40 μm thickness and mounted in a mixer block with waveguide dimensions of 120 by 240 μm and a cut-off frequency of 625 GHz scaled from a 345 GHz receiver[11]. The mixerblock is kept at about 4.5 K except for the measurement at the highest frequency where the temperature is approximately 3 K. A contacting backshort is used as a mechanical tuning element. Mylar beamsplitters of 15 and 20 μm thickness are used to couple in the local oscillator power. The vacuum window consists of 75 μm thick Mylar, a 110 μm black polyethylene sheet at 77 K functions as IR heat filter. The junctions are connected via an integrated low-pass filter and a circulator with 0.5 dB loss to the IF amplifier chain with a noise temperature of 3 K and 80 dB gain at 1.5 GHz with 85 MHz bandwidth.

3.3 Heterodyne measurements

The center frequency and bandwidth of the junction with stripline is measured using a Fourier transform spectrometer with different backshort positions. The measurements are shown in Fig. 3.1. The figure shows that with the aid of the
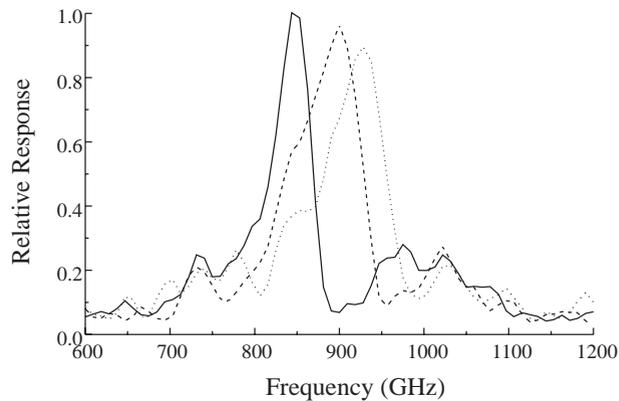

FIGURE 3.1. Fourier Transform Spectroscopy (FTS) spectrum for three different backshort positions. The vertical scale is normalized to the best response at 850 GHz for which the junction was designed. The peak height decreases with frequency because of the increasing absorption in the stripline and waveguide.

backshort the resonance frequency can be tuned from 800 to 1000 GHz. Beyond this frequency the response becomes too poor to be accurately measured.

Receiver noise measurements have been performed at 820, 903, and 979 GHz using standard hot/cold loads. For each frequency the bias voltage, backshort position and local oscillator power is adjusted to give optimum performance. Fig. 3.2b shows the IF output power at 820 GHz versus bias voltage for input powers corresponding to 77 K and 293 K.
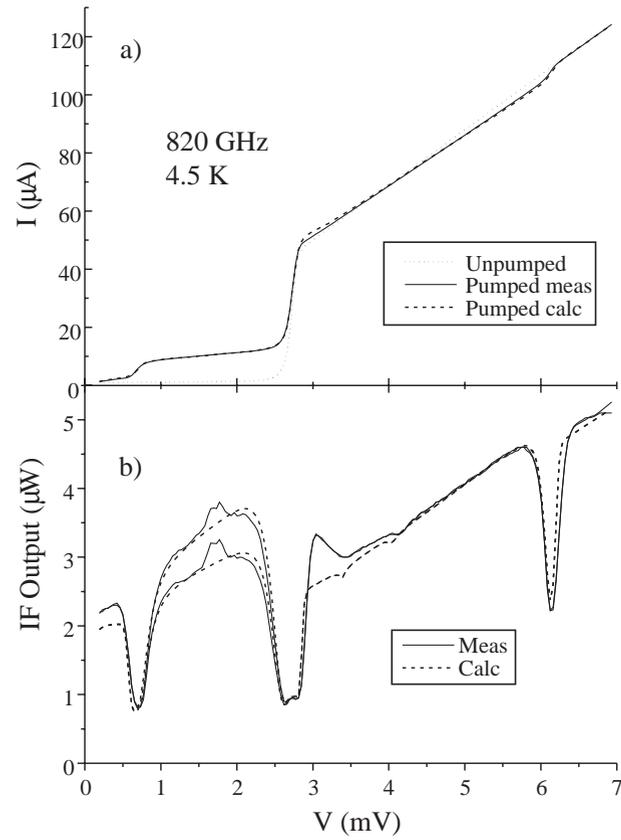
FIGURE 3.2.   **a.** Pumped, unpumped and calculated I,V curves. The pump frequency is 820 GHz. **b.** Measured and calculated IF output power for hot and cold loads. The peaks in the measured IF curves at the first photon step is due to incomplete suppression of the ac Josephson effect by a magnetic field. The peak corresponds to the position of the first Shapiro step at $hf/2e = 1.7$ mV. This leads to a decreased response as shown in Fig. 3.3.

The Y-factor (= P_{out}(hot)/P_{out}(cold)) and the receiver gain ($\propto P_{out}$(hot) − P_{out}(cold)) are shown in Fig. 3.3. The maximum Y-factor at 820 GHz is 0.86 dB, resulting in an uncorrected receiver noise temperature of 940 K using the full Planck's law. The uncorrected receiver noise temperatures at 903 and 979 GHz are 1040 and 1388 K.
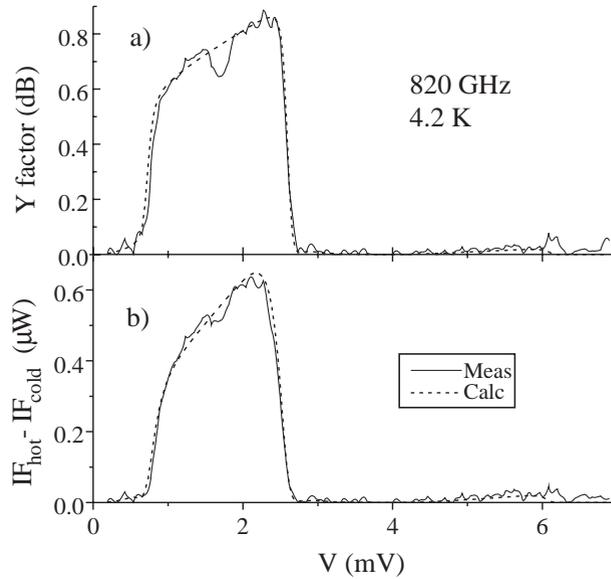

FIGURE 3.3. **a).** Measured and calculated Y-factor. **b).** Measured and calculated IF output power difference indicating the region with finite gain.

3.4 Receiver noise analysis

To examine the noise contribution of the separate receiver elements, the IF output power is calculated from the gain and noise of each element. The IF output power

is given by

$$P_{out} = k_B G_{IF} B((\frac{T_M}{2} + T_{qf} + T_{in})2 G_M G_{iso} + T_{IF}) \tag{3.1}$$

G_{IF} is the IF gain, determined by the shot noise method. B is the bandwidth of the IF filter and is measured by a spectrum analyzer. The single side band (SSB) mixer noise temperature T_M to be defined in (3.2) below is divided by 2 since the receiver is used as a double side band (DSB) receiver. The power contribution $\hbar\omega/2$ from the zero-point quantum fluctuations of both the image and the signal port is denoted by $k_B T_{qf}$. The power $k_B T_{in}$ of the signal is the effective power incident on the junction and is corrected for the loss in the high frequency input (RF) part of the receiver. G_M is the DSB gain of the mixer, to be defined in (3.3), G_{iso} that of the isolator between the junction and IF input port. The noise temperature T_{IF} of the cooled IF amplifier is corrected for the noise contribution of the isolator due to the impedance mismatch between the mixer and the IF amplifier input.

3.4.1   RF components

The measured numbers for the gain (transmission) of the RF elements are given in Table 3.1. Each element adds a power corresponding to its own physical temperature to the transmitted power by $P_{out} = P_{in} \cdot G_{element} + P_{phys} \cdot (1 - G_{element})$. P_{phys} is the black-body power calculated from the physical temperature of the element. The gain values include reflection and absorption losses. The gain of the lens, horn and waveguide is taken equal to those from separate measurement results of a 345 GHz mixer block[11]. The stripline loss is calculated as described in [7] using the Reuter-Sondheimer equation for the surface impedance in the extreme anomalous limit.

3.4.2   Mixer characteristics

The mixer performance is determined mainly by the I,V characteristics, the mismatch between the mixer input port and embedding impedance and the mismatch between the mixer output and IF amplifier input impedance. The embedding impedance is obtained by the voltage match method[12]. Although it requires a few numerical computations it provides reliable impedance values in agreement with results from scale model measurements[11]. We have assumed that since

TABLE 3.1. Gain of RF components

Component	820 GHz -dB	903 GHz -dB	979 GHz -dB
Beamsplitter	0.8	0.6	0.7
Dewar Window	1.0	0.8	0.6
Heat Filter	0.2	0.3	0.5
Lens + Horn	0.2	0.2	0.2
Stripline	8.0	8.2	8.9
Total G_{RF}	10.5	10.2	10.8

the matching to the junction by the stripline is rather poor, the upper and lower sidebands have equal impedances. The derived embedding admittance $Y_{emb} = G_{emb} + iB_{emb}$ normalized to the junction admittance is for all three frequencies $Y \cdot R_N = 1.4 + 0.5i$ indicating that the intrinsic capacitance of the junction is well tuned out by the combination of backshort and stripline. This value of the admittance is used in the three-port Tucker mixer model to obtain the mixer shot noise and gain listed in table 3.2 together with the values measured at the bias voltage of lowest receiver noise temperature. The SSB shot noise temperature of

TABLE 3.2. Mixer gain and noise

Frequency	T_M (calc) (K)	T_M (meas) (K)	G_M (calc) -dB	G_M (meas) -dB
820 GHz	31	51	9.0	9.5
903 GHz	34	69	9.9	10.3
979 GHz	29	74	9.3	9.6

a DSB receiver is given by[4]

$$T_M = \frac{G_L}{G_M k_B} \sum_{i=-1}^{1} \sum_{j=-1}^{1} Z_{0i} Z_{0j}{}^* H_{ij} \tag{3.2}$$

in which G_L is the $0.02\,\Omega^{-1}$ input conductance of the IF amplifier. $Z_{i,j}$ is the 3 x 3 conversion matrix linearly relating the currents i_j and voltages v_i at the relevant frequencies by $v_i = Z_{ij}i_j$. H_{ij} is the current correlation matrix accounting for the generation of thermal and shot noise, and the mutual correlation between noise at the different frequencies. The DSB gain G_M of the mixer is defined as the ratio of the incoming power and the power delivered to the IF amplifier and can be written as

$$G_M \;=\; 4G_L G_{emb}\mid Z_{01}\mid^2 \tag{3.3}$$

the Z_{01} coupling the input current to the output voltage. The values for the measured noise and gain in Table 3.2 are obtained by comparing (3.1) to the measured IF output power using G_M and T_M as unknowns.

3.5   Discussion and conclusions

From the good agreement between the measured and calculated IF output powers and resulting noise temperature and gain, we can conclude that the measured and calculated properties of the individual RF components in Table 3.1 constitute a convincing model for the receiver as a whole. The measured mixer noise temperatures presented in Table 3.2 are higher than expected from theory. The higher mixer noise temperature at 979 GHz may be due to a strong water absorption line. In earlier work[6],[11] the calculated mixer noise had to be raised as well, partly due to a relatively high subgap current. In our present high quality junctions this contribution should match theory. The derived mixer gains are close to the theoretical ones, therefore we can exclude a severe loss in the room temperature part of the receiver. An additional examination of the noise contribution of the ensemble of RF components[13] as opposed to simply adding those of the individual parts is needed to empirically disentangle the losses in the parts at room temperature and those at 77 or 4.2 K.

   The aim here is to establish which receiver parts contribute predominantly to the total noise temperature and to examine whether those contributions can be reduced. To do so, (3.1) is rewritten into

$$T_{REC} = T_{OPT} + \left[\frac{T_M + 2T_{qf}}{2} + \frac{T_{IF}}{2G_M G_{iso}} \right] \frac{1}{G_{RF}} \tag{3.4}$$

Herein is T_{OPT} the contribution of the room temperature parts of the RF input section which is small since the transmissions of those parts are close to the optimum

values . Equation 3.4 shows that the receiver noise temperature is linearly related to the RF loss, to which the stripline contributes most (G_{strip} = -8 dB of the total G_{RF} = -10.5 dB at 820 GHz). The mixer noise T_M is small since the junction quality is high. Improving the mixer gain G_M would merely reduce the relatively small noise contribution of the IF chain (the last term in (3.4)). Hence the obvious choice to lower the receiver noise temperature is to reduce the stripline loss. This loss is somewhat influenced by the material properties of the Al layer, but a major reduction can be expected from optimizing the microwave coupling design. Even though a series resonant circuit as we use can match both real and imaginary part of the junction impedance to the antenna, the inherent large impedance transformation ratio results in a significant loss if normal metals are used. In this respect it is useful to examine the results of Bin *et al*[9],[15] who use a parallel resonant circuit, resulting in a coupling which is almost a factor two higher. For comparison the values of the coupling and corrected receiver noise temperature from [9] are given in Table 3.3 together with our results.

TABLE 3.3.   Receiver noise temperature vs. stripline loss

Frequency	measured		Bin		NbN	
	G_{strip}	T_{REC}	G_{strip}	T_{REC}	G_{strip}	T_{REC}
	-dB	(K)	-dB	(K)	-dB	(K)
820 GHz	8.0	720	5.2	846	9.2	930
903 GHz	8.2	840			11.5	1700
979 GHz	8.9	890	5.2	938	13	2240

From the listed receiver noise temperatures it is clear that even though the stripline coupling is a factor two larger than the value we obtained, the resulting receiver noise temperatures are not twice as good as ours, in fact they are slightly worse. We conjecture that this reflects the different junction qualities. The junction $R_{(2mV)}/R_N$ in [9] is 7 whereas our junctions have a ratio of 25. It has been shown theoretically that depending on the embedding impedance, a doubling of an already significant subgap current can result in a factor 1.5 increase in the mixer noise temperature T_M and an equal decrease of the mixer gain G_M[3]. This dependence of T_M and G_M on the subgap current apparently doubles the term in brackets in (3.4), canceling the effect of an increased stripline coupling and effec-

tively offering no sensitivity improvement.

Assuming that this analysis is correct we predict that for optimized receivers a T_{REC} of 600 K at 1 THz is attainable.

The numbers for the NbN stripline loss in Table 3.3 were obtained using surface resistance values for polycrystalline NbN[14]. From the resulting receiver noise temperatures it is apparent that polycrystalline NbN is not suitable as low loss stripline material. The surface resistance is higher than that of a normal metal except at lower frequencies, where Nb will be the most obvious choice.

To summarize, we have analyzed the performance of a Nb tunnel junction embedded in an Al tuning circuit in the frequency range of 0.8 to 1 THz. The main limitation to the receiver sensitivity appears to be the loss in the normal metal tuning circuit. In the near future the main sensitivity improvement can be expected from a design focussed on low loss circuits employing high quality, high current density junctions rather than putting effort into stripline materials choice and optimization.

References

[1] A.V. Räisänen, W.R. Mc.Grath, P.L. Richards, and F.L. Lloyd, *IEEE Trans. Microwave Theory Techn.*, vol. 33, p. 1495, 1985.

[2] D. Winkler and T. Claeson, *J. Appl. Phys.*, vol. 62, pp. 4482-4498, 1987.

[3] W.C. Danchi and E.C. Sutton, *J. Appl. Phys.*, vol. 60, pp. 3967-3977, 1986.

[4] J.R. Tucker, M.J. Feldman, *Rev. Mod. Phys.*, vol. 57, pp. 1055-1113, 1985.

[5] M.C. Gaidis, H.G. LeDuc, M. Bin, D. Miller, J.A. Stern, and J. Zmuidzinas, unpublished.

[6] G. de Lange, C.E Honingh, J.J. Kuipers, H.H.A Schaeffer, R.A. Panhuyzen, T.M. Klapwijk, H. van de Stadt, and M.W.M. de Graauw, *Appl. Phys. Lett.*, vol. 64, pp. 3039-3041, 1994.

[7] G. de Lange, J.J. Kuipers, T.M. Klapwijk, R.A. Panhuyzen, H. van de Stadt, and M.W.M. de Graauw, *J. Appl. Phys.*, vol. 77, pp. 1795-1804, 1995.

[8] H. van de Stadt et al, *Sixth Int. Symp. on Space THz Techn.*, March 1995, CalTech. Pasadena, California, USA.

[9] M. Bin, M.C. Gaidis, J. Zmuidzinas, T.G. Phillips, H.G. LeDuc, *Appl. Phys. Lett.*, vol. 68, pp. 1714-1716, 1996.

[10] J.R. Gao, S. Kovtonyuk, J.B.M. Jegers, P. Dieleman, T.M. Klapwijk, and

H. van de Stadt, *Seventh Int. Symp. on Space THz Techn.*, March 1996, Charlottesville, USA.

[11] C.E. Honingh et al, *J. Appl. Phys.*, vol. 74, pp. 4762-4773, 1993.

[12] A. Skalare, *Int. J. of IR and MM Waves*, vol. 10, pp. 1339-1353, 1989.

[13] R. Blundell, R.E. Miller, and K.H. Gundlach, *Int. J. of IR and MM Waves*, vol. 13, pp. 3-14, 1992.

[14] S. Kohjiro, S. Kiryu, and A. Shoji, *IEEE Trans. Appl. Supercond.*, vol. 3, pp. 1765-1767, 1993.

[15] M. Bin, M.C. Gaidis, D. Miller, J. Zmuidzinas, T.G. Philips, and H.G. LeDuc, *Seventh Int. Symp. on Space THz Techn.*, March 1996, Charlottesville, USA.